



# PCCP

**A Vacuum Ultraviolet Photoionization Study on the Formation of Methanimine ( $\text{CH}_2\text{NH}$ ) and Ethylenediamine ( $\text{NH}_2\text{CH}_2\text{CH}_2\text{NH}_2$ ) in Low Temperature Interstellar Model Ices Exposed to Ionizing Radiation**

Journal:	<i>Physical Chemistry Chemical Physics</i>
Manuscript ID	CP-ART-09-2018-006002.R2
Article Type:	Paper
Date Submitted by the Author:	19-Dec-2018
Complete List of Authors:	Zhu, Cheng; University of Hawaii, Department of Chemistry Frigge, Robert; University of Hawaii, Department of Chemistry Turner, Andrew; University of Hawaii, Abplanalp, Matthew; University of Hawaii, Sun, Bing-Jian; National Dong Hwa University, Department of Chemistry Chen, Yue-Lin; National Dong Hwa University, Department of Chemistry Chang, Agnes; National Dong Hwa University, Department of Chemistry Kaiser, Ralf I; University of Hawaii,

SCHOLARONE™  
Manuscripts

# **A Vacuum Ultraviolet Photoionization Study on the Formation of Methanimine ( $\text{CH}_2\text{NH}$ ) and Ethylenediamine ( $\text{NH}_2\text{CH}_2\text{CH}_2\text{NH}_2$ ) in Low Temperature Interstellar Model Ices Exposed to Ionizing Radiation**

Cheng Zhu,<sup>‡ab</sup> Robert Frigge,<sup>‡ab</sup> Andrew M. Turner,<sup>ab</sup> Matthew J. Abplanalp,<sup>ab</sup> Bing-Jian Sun,<sup>c</sup>  
Yue-Lin Chen,<sup>c</sup> Agnes H. H. Chang<sup>c</sup> and Ralf I. Kaiser<sup>\*ab</sup>

<sup>a</sup> W. M. Keck Research Laboratory in Astrochemistry, University of Hawaii at Manoa, Honolulu, Hawaii 96822, USA; [ralfk@hawaii.edu](mailto:ralfk@hawaii.edu)

<sup>b</sup> Department of Chemistry, University of Hawaii at Manoa, Honolulu, Hawaii 96822, USA

<sup>c</sup> Department of Chemistry, National Dong Hwa University, Shoufeng, Hualien 974, Taiwan

<sup>‡</sup> These authors contributed equally.

### Abstract

Methylamine ( $\text{CH}_3\text{NH}_2$ ) and methanimine ( $\text{CH}_2\text{NH}$ ) represent essential building blocks in the formation of amino acids in interstellar and cometary ices. In our study, by exploiting isomer selective detection of the reaction products via photoionization coupled with reflectron time of flight mass spectrometry (Re-TOF-MS), we elucidate the formation of methanimine and ethylenediamine ( $\text{NH}_2\text{CH}_2\text{CH}_2\text{NH}_2$ ) in methylamine ices exposed to energetic electrons as a proxy for secondary electrons generated by energetic cosmic rays penetrating interstellar and cometary ices. Interestingly, the two products methanimine and ethylenediamine are isoelectronic to formaldehyde ( $\text{H}_2\text{CO}$ ) and ethylene glycol ( $\text{OHCH}_2\text{CH}_2\text{OH}$ ), respectively. Their formation has been confirmed in interstellar ice analogs consisting of methanol ( $\text{CH}_3\text{OH}$ ) which is isoelectronic to methylamine. Both oxygen-bearing species formed in methanol have been detected in the interstellar medium (ISM), while for methanimine and ethylenediamine only methanimine has been identified so far. In comparison with the methanol ice products and our experimental findings we predict that ethylenediamine should be detectable in those astronomical sources, where methylamine and methanimine are present.

Keywords: astrochemistry, cosmic rays, ISM: molecules, methods: laboratory: solidstate, molecular processes, radiation mechanism: non-thermal

## 1. Introduction

During the last decades, the methanimine molecule ( $\text{CH}_2\text{NH}$ ) has received considerable attention from the astrochemistry and the astronomy communities due to its role as a potential precursor in the abiotic formation of amino acids such as glycine ( $\text{NH}_2\text{CH}_2\text{COOH}$ ) - the simplest amino acid<sup>1, 2</sup> - in the interstellar medium (ISM). Although more than 80 amino acids were identified in carbonaceous chondrites like in the Murchison meteorite<sup>3</sup> and recently glycine in the comet 81P/Wild 2,<sup>4</sup> the understanding of their fundamental formation mechanisms is still in its infancy.<sup>5-10</sup> Glycine, alanine ( $\text{CH}_3\text{CH}(\text{NH}_2)\text{COOH}$ ), valine ( $((\text{CH}_3)_2\text{CHCH}(\text{NH}_2)\text{COOH}$ ), proline ( $\text{c}-(\text{NHCH}_2\text{CH}_2\text{CH}_2\text{CH})\text{COOH}$ ), serine ( $\text{OHCH}_2\text{CH}(\text{NH}_2)\text{COOH}$ ), and aspartic acid ( $\text{OHC}(\text{O})\text{CH}_2\text{CH}(\text{NH}_2)\text{COOH}$ ) were identified *via* chromatography in the room temperature residues of irradiated interstellar ice analogues containing water ( $\text{H}_2\text{O}$ ), ammonia ( $\text{NH}_3$ ), methanol ( $\text{CH}_3\text{OH}$ ), hydrogen cyanide ( $\text{HCN}$ ), carbon monoxide ( $\text{CO}$ ), and carbon dioxide ( $\text{CO}_2$ )<sup>10-13</sup>. These results elucidated a radiation induced low temperature formation pathway toward glycine commencing with the decomposition of methylamine ( $\text{CH}_3\text{NH}_2$ ) *via* production of  $\text{CH}_2\text{NH}_2$  together with suprathreshold hydrogen atoms. The latter react with  $\text{CO}_2$  to form the hydroxycarbonyl radical ( $\text{HOCO}$ ), which then recombines with the aminomethyl radicals ( $\text{CH}_2\text{NH}_2$ ) to form glycine. This pathway was also supported by quantum chemistry calculations.<sup>14</sup> Alternatively, Kaiser et al.<sup>10</sup> discussed a formation pathway toward glycine ( $\text{NH}_2\text{CH}_2\text{COOH}$ ) *via*  $\text{NH}_3$  and acetic acid ( $\text{CH}_3\text{COOH}$ ) - the latter which was previously detected in irradiated  $\text{CO}_2$  and methane ( $\text{CH}_4$ ) ices<sup>15, 16</sup> - *via* radical - radical recombination of radiolytically generated amino ( $\text{NH}_2$ ) and hydroxycarbonylmethyl radicals ( $\text{CH}_2\text{COOH}$ ).

The  $\text{CH}_2\text{NH}$  molecule itself - also called formalimine due to the isoelectronic structure with formaldehyde ( $\text{H}_2\text{CO}$ ) - was first detected in the hot core Sagittarius B2 toward the galactic center through the 64-m radio telescope *via* the  $1_{10-1_{11}}$  multiplet<sup>17</sup> with a column density of  $3 \times 10^{14} \text{ cm}^{-2}$ . Follow up searches consolidate this finding<sup>18-22</sup> and confirmed the presence of  $\text{CH}_2\text{NH}$  in L183,<sup>23</sup> Orion-KL,<sup>1, 24</sup> W51, Orion 3N, G34.3+0.15,<sup>1</sup> and G19.61-0.23,<sup>25</sup> as well as in the circumstellar shell of IRC+10216.<sup>26</sup> Methanimine was also detected in the ultraluminous infrared galaxy Arcebo ARP 220.<sup>27</sup> In the solar system, the atmosphere of Saturn's moon Titan also reveals an abundance of  $\text{CH}_2\text{NH}$  as discovered by the Cassini T5 flyby.<sup>28</sup> Furthermore, methylamine has been detected in dust samples collected by the Stardust mission<sup>4</sup> and was

recently also observed on the comet 67P/Churyumov-Gerasimenko.<sup>29</sup> In summary we can find CH<sub>2</sub>NH in every environment in the interstellar medium which underlines its importance in the interstellar chemistry.

However, despite the potential importance of CH<sub>2</sub>NH, the underlying formation pathways are still not resolved. In the gas phase, bimolecular neutral-neutral reactions of methyldidyne (CH) with NH<sub>3</sub> have been proposed to synthesize CH<sub>2</sub>NH along with atomic hydrogen (H).<sup>26</sup> In laboratory experiments, Michael et al.<sup>30</sup> detected traces of CH<sub>2</sub>NH through photolysis of CH<sub>3</sub>NH<sub>2</sub> by non-monochromatic ultra violet (UV) radiation around 220 nm. However, formation rates through these pathways are too low and cannot explain the observed fractional abundances of CH<sub>2</sub>NH in the interstellar medium.<sup>23, 31</sup> For instance, toward the cold cloud L183, fractional abundances of CH<sub>2</sub>NH were detected at levels of  $8.1 \times 10^{-10}$ ,<sup>1, 23</sup> but astrochemical models predict fractional abundances about one to two orders of magnitude below the actual observations. Therefore, gas phase chemistry alone cannot account for the formation of interstellar CH<sub>2</sub>NH, and critical production routes are still lacking.

An alternative source for CH<sub>2</sub>NH can be found in formation routes in condensed matter, i.e. within interstellar ices containing NH<sub>3</sub> and CH<sub>4</sub> exposed to ionizing radiation. Here, methanimine has been detected tentatively in broad band ultraviolet (UV) irradiated interstellar model ices carrying CH<sub>4</sub> and NH<sub>3</sub>.<sup>32, 33</sup> Photolysis of CH<sub>3</sub>NH<sub>2</sub> ice has also been studied by Bossa et al.<sup>34</sup> tentatively assigning CH<sub>2</sub>NH *via* its symmetric C-H stretch vibration at 3144 cm<sup>-1</sup> appearing as a shoulder of the hydrogen-bonding mode of the CH<sub>3</sub>NH<sub>2</sub> parent. Woon et al.<sup>14</sup> discussed the formation of CH<sub>2</sub>NH along with CH<sub>3</sub>NH<sub>2</sub> *via* a sequential hydrogenation of HCN, which was confirmed experimentally, by Theule et al.<sup>35</sup> Kim et al.<sup>36</sup> demonstrated that a radical-radical recombination between methyl (CH<sub>3</sub>) and amide (NH<sub>2</sub>) in CH<sub>4</sub> – NH<sub>3</sub> bearing ices followed by radiolysis leads ultimately to HCN *via* CH<sub>3</sub>NH<sub>2</sub> and CH<sub>2</sub>NH intermediates.

The aforementioned considerations revealed that an experimental elucidation of the synthetic pathways to CH<sub>2</sub>NH in low temperature interstellar analog ices exposed to ionizing radiation is still in its infancy. Nevertheless, they provide a significant potential to account for the missing CH<sub>2</sub>NH source in the ISM. Previously analytical techniques attempted to detect CH<sub>2</sub>NH *via* low temperature Fourier Transform Infrared Spectroscopy (FTIR) of the exposed ices.<sup>34</sup> Additionally, a quadrupole mass spectrometry (QMS) coupled with electron impact ionization has been used in

that study to probe CH<sub>2</sub>NH subliming in the post irradiation phase into the gas phase. These approaches hold significant complications. FTIR spectroscopy represents an ideal tool to investigate the processing and decay kinetics of ‘small’ molecules such as CO, H<sub>2</sub>O, CH<sub>3</sub>OH, CO<sub>2</sub>, CH<sub>4</sub>, H<sub>2</sub>CO, along with NH<sub>3</sub> – those molecules have been detected on interstellar grains. However, the ability of infrared spectroscopy to provide useful information for the detection of complex organics formed within the ices is quite limited. Infrared spectroscopy allows the identification of *functional groups* of organics. This information does not always identify individual molecules since the functional groups of, for instance, amines (R–NH<sub>2</sub>) and imine (RHC=NH) portray similar group frequencies in the range of 1650 cm<sup>-1</sup> to 1500 cm<sup>-1</sup> and 3500 cm<sup>-1</sup> to 3300 cm<sup>-1</sup>.<sup>37</sup> Therefore, the exclusive assignment of a newly formed molecule based on infrared bands in an unknown mixture of organics is rarely scientifically sound. Using QMS coupled with electron impact ionization to ionize the subliming molecules of the irradiated ices during the temperature programmed desorption (TPD) exploits often an electron impact ionizer operating at 70 to 100 eV electron energy. This energy range does not only ionize molecules, but also results in a significant fragmentation of the parent ion. This might even result in the absence of the molecular parent ion. Furthermore, the fragment ions of structural isomers often overlap making it difficult to decipher or even to discriminate between structural isomers. The exploitation of soft ionization with low energy electrons of a few electron volt kinetic energy has a few advantages. However, a voltage drop across the filaments of typically 1.0 eV results in electrons with a relatively broad energy distribution thus making it difficult to selectively ionize structural isomers. Therefore, alternative analytical techniques are required to elucidate the formation of CH<sub>2</sub>NH in low temperature interstellar ice analogues.

In this work, we use single photon ionization (PI) coupled with a reflection time-of-flight mass spectrometer (ReTOF-MS) to detect and to distinguish structural isomers of organic molecules subliming into the gas phase during temperature programmed desorption (TPD) after exposing the ices to ionizing radiation. In comparison to traditional electron impact ionization, PI-ReTOF-MS – utilizing photon energies close to the ionization threshold of the molecules – forms gas phase ions without significant internal energy and hence ideally without fragmentation.<sup>38, 39</sup> Likewise, employing distinct photon energies of 9.93 eV, 9.10 eV, and 8.17 eV as conducted in the present work, this technique can be utilized to *selectively discriminate between structural isomers* of organic molecules as previously demonstrated.<sup>40</sup> The

present study demonstrates for the first time unambiguously that CH<sub>2</sub>NH can be synthesized in low temperature (5 K) interstellar model ices of CH<sub>3</sub>NH<sub>2</sub>, when exposed to ionizing radiation such as energetic electrons. These energetic electrons simulate secondary electrons released during the passage of galactic cosmic rays through interstellar ices.<sup>41</sup> The present laboratory simulation experiments mirror the exposure of the interstellar ices in molecular clouds by galactic cosmic rays during a life time of a molecular cloud of typically 10<sup>5</sup> years. Considering that molecular clouds constitute the nurseries of stars and planetary systems,<sup>42-44</sup> the identification of CH<sub>2</sub>NH along with ethylenediamine (NH<sub>2</sub>CH<sub>2</sub>CH<sub>2</sub>NH<sub>2</sub>) in our experiments suggests that these molecules may have been at least partially incorporated into our Solar System from interstellar matter *via* circumstellar disks. Finally, considering the isoelectronicity between CH<sub>3</sub>NH<sub>2</sub> and CH<sub>3</sub>OH, the formation pathways of the CH<sub>2</sub>NH and NH<sub>2</sub>CH<sub>2</sub>CH<sub>2</sub>NH<sub>2</sub> molecules are compared to those of the H<sub>2</sub>CO and ethylene glycol (OHCH<sub>2</sub>CH<sub>2</sub>OH) in interstellar model ices exposed to ionizing radiation.<sup>41, 45-47</sup>

## 2. Experimental Methods

The experiments were performed at the W. M. Keck Research Laboratory in Astrochemistry. The experimental setup consists of a contamination-free stainless steel ultra-high vacuum chamber (UHV) operated at a base pressure of a few 10<sup>-11</sup> Torr backed by turbo molecular pumps and dry oil-free scroll pumps. A polished polycrystalline silver mirror within the chamber is coupled to a cold finger cooled to 5.5 ± 0.1 K using a UHV compatible closed-cycle helium compressor (Sumitomo Heavy Industries, RDK-415E). The target can be moved in two degrees of freedom, translation in the vertical axis and rotation in the horizontal plane. Methylamine gas (Sigma Aldrich; 99 %) was deposited onto the cooled silver wafer *via* a glass capillary at a base pressure of 5.5 × 10<sup>-9</sup> Torr for 7 min until the desired ice thickness was achieved. This ice growth was monitored online and *in situ* *via* laser interferometry measurements. In this method, the HeNe laser ( $\lambda = 632.8$  nm; CVI Melles-Griot; 25-LHP-230) reflections of the silver mirror and the ice surface introduce an interference pattern. The beam was reflected into a photodiode and the pattern is measured with a picoammeter (Keithley 6485). The recorded fringes result in the thickness of the ice *via* equation (1), which describes the thickness ( $d$ ) of an ice in dependence of the number of interference fringes ( $m$ ), the laser wavelength ( $\lambda$ ), and the angle of incidence of the laser beam ( $\theta = 4^\circ$ ).<sup>48-50</sup>

$$d = \frac{m\lambda}{2\sqrt{n^2 - \sin^2 \theta}} \quad (1)$$

A refractive index ( $n$ ) for  $\text{CH}_3\text{NH}_2$  ice of  $1.40 \pm 0.3$  is derived from the density ( $\rho = 0.785 \text{ g cm}^{-3}$ ) and refractive index ( $n_f = 1.371$ ) of liquid  $\text{CH}_3\text{NH}_2$  via the Lorentz-Lorentz relation<sup>51, 52</sup> with the Lorenz coefficient ( $L$ ) to be constant over a fixed wavelength:

$$L\rho = \frac{n_f^2 - 1}{n_f^2 + 2} \quad (2)$$

With the density of  $\text{CH}_3\text{NH}_2$  ice of  $\rho = 0.85 \text{ g cm}^{-3}$ ,<sup>53, 54</sup> the thickness of the prepared  $\text{CH}_3\text{NH}_2$  ice is  $200 \pm 50 \text{ nm}$ . After the deposition with a rate of  $30 \pm 5 \text{ nm min}^{-1}$ , an area of  $1.0 \pm 0.1 \text{ cm}^2$  of  $\text{CH}_3\text{NH}_2$  ice was then irradiated by an electron gun (specs, PU-EQ22) with 5 keV electrons for 15 min with an electron current of 20 nA at an angle of incidence of  $70^\circ$  relative to the surface normal. Galactic cosmic rays (GCR) consist mainly of protons with kinetic energy up to PeV. Interacting with interstellar ices and ionizing of molecules lead to an energy loss of the GCRs and result in secondary electron which subsequently ionize further molecules generating electron cascades with energies in the range of eV – keV.<sup>55</sup> Therefore, the 5 keV electrons mimic efficiently the irradiation by GCRs. By utilizing CASINO 2.42 software<sup>56</sup> an average penetration depth of  $180 \pm 80 \text{ nm}$  is achieved (Table S1). The average dose absorbed is determined to be  $1.0 \pm 0.1 \text{ eV molecule}^{-1}$ . During the irradiation the chemical evolution of the  $\text{CH}_3\text{NH}_2$  ice was monitored online and *in situ* using FTIR (Nicolet 6700, MCT-A) in the range of  $4500 \text{ cm}^{-1} - 500 \text{ cm}^{-1}$ , with a resolution of  $4 \text{ cm}^{-1}$ , at a reflection angle of  $45^\circ$  for absorption-reflection-absorption mode. Once the irradiation was completed, the ice was held at 5.5 K for additional 30 min before starting temperature programmed desorption (TPD) by heating the substrate from 5.5 K to 320 K at a rate of  $0.5 \text{ K min}^{-1}$ .

To detect the subliming molecules with the PI-ReTOF-MS, the neutral molecules are subliming during TPD and are ionized by pulsed vacuum ultraviolet (VUV) laser light close to 2 mm in front of the ice sample. The ions produced are mass-resolved and detected by a multichannel plate in a dual chevron configuration and then amplified by a fast preamplifier (Ortec 9305) and shaped with a 100 MHz discriminator. Finally, the spectra are recorded using a computer-controlled multichannel scaler (FAST ComTec, P7888-1E) with 4 ns bin widths



triggered at 30 Hz using a pulse delay generator (Quantum Composer, 9518) and 3600 sweeps per mass spectrum per 1 K increase in temperature during TPD.

The VUV radiation is generated by difference-frequency mixing ( $2\omega_1 - \omega_2$ ) in a noble gas (krypton (Kr), xenon (Xe)) using two dye lasers (Sirah Lasertechnik, Model Cobra-Stretch, and Precision Scan) each pumped with a Nd:YAG laser (Spectra-Physics, Models PRO-270-30). The laser wavelengths were measured using a WaveMaster laser wavelength meter (COHERENT). In order to record and monitor the VUV light a detection system consisting of a Faraday cup and a diode calibrated by the national institute of standards and technology (NIST) is placed behind the detection region. This tunable VUV photon source allows soft-ionization of molecules with almost no fragmentation.<sup>40</sup> In this work we used a mixture of Rhodamine 610 and Rhodamine 640 in the first dye laser, pumped with 532 nm, to generate 606.948 nm, which is frequency tripled to  $\omega_1 = 202.316$  nm for the two-photon resonance of krypton (Kr). Adding the second laser at a wavelength of  $\omega_2 = 532$  nm results in the VUV energy of 9.93 eV (124.9 nm). For the second VUV energy of 9.10 eV the first dye laser with Coumarin 450 as dye is pumped with 355 nm to achieve 445.132 nm which result in  $\omega_1 = 222.566$  nm by frequency doubling for the two-photon resonance in xenon (Xe). The second dye laser with Rhodamine 610 / Rhodamine 640 is pumped with 532 nm to generate 607 nm. The final photoionization energy used is 8.17 eV (151.8 nm). It is generated by difference frequency mixing of  $\omega_1 = 249.628$  nm and  $\omega_2 = 703$  nm in xenon gas (Xe). The first dye laser is prepared with Coumarin 503 and pumped with 355 nm to achieve a wavelength of 499.265 nm before frequency doubling. The second wavelength is generated by the laser dye LDS 867 pumped with 532 nm. An overview of the photon ionization energies and their preparation can be found in Table 1. Calibration measurements for the ReTOF reveal a potential lowering of the ionization energies of the subliming molecules by up to 0.03 to 0.04 eV due to the static electric field induced Stark effect.<sup>57</sup> This has been confirmed by separately calibration experiments using molecules with known ionization potentials, such as methyl bromide ( $\text{CH}_3\text{Br}$ ) (IE =  $10.540 \pm 0.003$  eV<sup>58</sup>), dibromochloromethane ( $\text{CHBr}_2\text{Cl}$ ) (IE =  $10.59 \pm 0.01$  eV<sup>59</sup>) and hexafluoropropylene ( $\text{C}_3\text{F}_6$ ) (IE =  $10.60 \pm 0.03$  eV<sup>60</sup>).

### 3. Computational Methods

The hybrid density functional B3LYP<sup>61-64</sup> with the cc-pVTZ basis set was employed to optimize geometries and harmonic frequencies of the species and their cations. Afterwards, their coupled cluster<sup>65-68</sup> CCSD(T)/cc-pVDZ, CCSD(T)/cc-pVTZ, and CCSD(T)/cc-pVQZ energies were calculated and extrapolated to complete basis set limits,<sup>69</sup> CCSD(T)/CBS, with B3LYP/cc-pVTZ zero-point energy corrections. The energy difference between the ionic and neutral state with similar geometry gives the adiabatic ionization energy. The GAUSSIAN09 program<sup>70</sup> was utilized in the electronic structure calculations. Table 2 presents the calculated adiabatic ionization energies for two sets of isomers CNH<sub>3</sub> and C<sub>2</sub>N<sub>2</sub>H<sub>8</sub> along with the relative energies of the structural isomers considered in this study and ionization energy values from the literature. A comparison between theoretical and experimental results as a benchmark calculation reveals that the calculations overestimate the ionization energies by 0.03 eV to 0.05 eV.<sup>71-73</sup> Molecular geometries as well as vibrational modes for the CNH<sub>3</sub> and C<sub>2</sub>N<sub>2</sub>H<sub>8</sub> isomers are presented in the supplement material (Tables S2 and S3).

### 4. Results

Figure 1 presents the FTIR spectra of CH<sub>3</sub>NH<sub>2</sub> before (black line) and after (red line) the irradiation for the high (3500 – 2700 cm<sup>-1</sup>) and low (1700 – 800 cm<sup>-1</sup>) energy regions. All absorptions can be attributed to CH<sub>3</sub>NH<sub>2</sub> as presented by previous studies.<sup>34, 74</sup> Their assignments are compiled in Table 3. The region from 3400 to 3100 cm<sup>-1</sup> is governed by the NH<sub>2</sub> antisymmetric ( $\nu_1$ ) and symmetric ( $\nu_{10}$ ) stretching vibrations, while the region of 3000 - 2700 cm<sup>-1</sup> connects to the two degenerate ( $\nu_{11}, \nu_2$ ) and the symmetrical ( $\nu_3$ ) CH<sub>3</sub> stretching vibrations of CH<sub>3</sub>NH<sub>2</sub>. The multiple peak structures and peak shift of these modes are characteristic for Fermi resonances. The feature at 3170 cm<sup>-1</sup> is interpreted by Durig et al.<sup>74</sup> as hydrogen bonding to the nitrogen electron lone pair. At lower energies, features for the scissors ( $\nu_4$ ) mode of NH<sub>2</sub> and the degenerate ( $\nu_{12}, \nu_5$ ) and symmetric ( $\nu_6$ ) CH<sub>3</sub> deformations are visible followed by the very weak NH<sub>2</sub> twisting ( $\nu_{13}$ ). From 1250 cm<sup>-1</sup> the C–N ( $\nu_8$ ) stretching as well as the first overtone of the torsion ( $\nu_{15}$ ) can be found surrounded by the NH<sub>2</sub> wagging ( $\nu_9$ ) and CH<sub>3</sub> rocking ( $\nu_7, \nu_{14}$ ) modes. The modes found in this study agree with the findings of Durig et al.<sup>96</sup> as presented in Table 3.

For the irradiated sample, only minor differences can be detected considering the low irradiation dose of only  $1.0 \pm 0.2$  eV molecule<sup>-1</sup>. The intensities of the CH<sub>3</sub>NH<sub>2</sub> fundamental vibrations are reduced compared to the unirradiated sample by  $8 \pm 1$  % (average decrease of each fundamental band area), revealing that  $0.09 \pm 0.01$  CH<sub>3</sub>NH<sub>2</sub> molecules eV<sup>-1</sup> are reacting during the radiation exposure. In the region of 3000 - 3200 cm<sup>-1</sup>, a shoulder at 3140 cm<sup>-1</sup> becomes visible. This shoulder can be attributed tentatively to the antisymmetric C-H ( $\nu_{as}$ ) stretching mode of CH<sub>2</sub>NH.<sup>35</sup> A second shoulder can be found at 1635 cm<sup>-1</sup> in the NH<sub>2</sub> scissor mode ( $\nu_4$ ). This feature might be attributed to the C=N double bond stretching of CH<sub>2</sub>NH (Table 3). Further, new modes around 1650 cm<sup>-1</sup>, 1550 cm<sup>-1</sup>, and 1380 cm<sup>-1</sup> (blue arrows) could be addressed to several possible functional groups. Around 1650 cm<sup>-1</sup> mostly C=C and C=N stretching vibrations can be found, while features around 1550 cm<sup>-1</sup> are most likely associated with the amine functional group *via* NH<sub>2</sub> scissor or NH deformation. The features around 1380 cm<sup>-1</sup> are typical for alkane functional groups visible by CH deformation modes. The newly formed molecules consisting of C, N, and H can be attributed to these features. However, due to the weak appearance and overlaps of functional groups for different molecules, it is difficult to identify individual molecules. Taking into account the energy loss of the electrons while penetrating the ices (Table S1),  $(25 \pm 3) \times 10^{15}$  CH<sub>3</sub>NH<sub>2</sub> molecules are destroyed during irradiation in an area of 1 cm<sup>2</sup>. If each destroyed molecule is converted to CH<sub>2</sub>NH,  $0.09 \pm 0.01$  molecules of CH<sub>2</sub>NH are formed per eV. Naturally, this value can only be considered as an *upper limit* for the CH<sub>2</sub>NH formation, since other molecules are formed as well based on the observation of the aforementioned functional groups and the Re-TOF-MS data as discussed below. In conclusion, the FTIR results show the preparation and processing of CH<sub>3</sub>NH<sub>2</sub> ice. However only tentatively results can be found for the products formed.

Compared to FTIR, the PI-ReTOF-MS detection method is significantly more sensitive and can discriminate between structural isomers – information which hardly can be extracted by alternative techniques in astrophysical ice simulation experiments.<sup>16, 48, 75-77</sup> The PI-ReTOF-MS data are compiled in Figure 2 for distinct ionization energies of 9.93 eV, 9.10 eV, and 8.17 eV while corresponding TPD graphs for selected m/z ratios critical to the present study are presented in Figure 3. Figures 2a/b represent the PI-ReTOF-MS data of the unirradiated (blank) and of the irradiated ices, respectively, recorded with the highest photon energy of 9.93 eV. The most

intense signal in the control experiment and the irradiated ice sample appear at mass-to-charge ratios ( $m/z$ ) of 30, 31, 32, and 33 in the temperature range from 100 K to 120 K. The most intense ion counts as presented in Figure 3a can be attributed to the parent molecule  $\text{CH}_3\text{NH}_2$  ( $\text{CH}_3\text{NH}_2$ ; 31 amu;  $\text{IE} = 8.97 \pm 0.02$  eV).<sup>78, 79</sup> Since  $\text{CH}_3\text{NH}_2$  has an ionization energy of 8.97 eV, it cannot be observed at a photon energy of 8.17 eV (Figure 2d). For photon energies above 9 eV, the appearance of the ion at  $m/z = 30$  could be assigned to  $\text{CNH}_4^+$  ( $m/z = 30$ ), which results from atomic hydrogen loss of  $\text{CH}_3\text{NH}_2$  ( $\text{CH}_3\text{NH}_2$ ; 31 amu). Furthermore, the ion counts at  $m/z = 32$  can be explained by protonated  $\text{CH}_3\text{NH}_2$  ( $\text{CH}_3\text{NH}_3^+$ ) and the naturally occurring  $^{13}\text{C}$ -substituted  $\text{CH}_3\text{NH}_2$  ( $^{13}\text{CH}_3\text{NH}_2$ ); the protonated  $^{13}\text{C}$ -substituted  $\text{CH}_3\text{NH}_2$  ( $^{13}\text{CH}_3\text{NH}_3^+$ ) can be linked to  $m/z = 33$ . A noticeable smaller feature can be monitored in the pristine and irradiated systems at  $m/z = 45$  desorbing at the same temperature as  $\text{CH}_3\text{NH}_2$ . This signal can be attributed to ionized ethylamine ( $\text{CH}_3\text{CH}_2\text{NH}_2$ ) and/or dimethylamine ( $\text{CH}_3\text{NHCH}_3$ ). These molecules have ionization energies of 8.9 eV and 8.2 eV (Table 4), respectively, and can be attributed to tracer impurities in the  $\text{CH}_3\text{NH}_2$  gas (99 %). Furthermore, the ion signal at  $m/z = 59$  can be related to propylamine ( $\text{CH}_3\text{CH}_2\text{CH}_2\text{NH}_2$ ), 2-propanamine ( $(\text{CH}_3)_2\text{CHNH}_2$ ), and/or n-methyl ethanamine ( $\text{CH}_3\text{CH}_2\text{NHCH}_3$ ) which have ionization energies of 8.78 eV, 8.72 eV, and 8.15 eV, respectively (Table 4).

After the irradiation, several new mass-to-charge ratios were observed, which were absent in the blank experiment. The TPD traces are presented in Figure 3. Due to the simplicity of the ice, the resulting molecules after the irradiation can only be composed of three elements: hydrogen (H), nitrogen (N), and carbon (C). The new signal at  $m/z = 29$  appearing between 106 K and 124 K can only be explained by four different isomers of  $\text{CNH}_3$ :  $\text{CH}_2\text{NH}$ ,  $\text{CHNH}_2$ , triplet methylimidogen ( $^3\text{CH}_3\text{N}$ ), and triplet aminomethylene ( $^3\text{CHNH}_2$ ) (Table 2). The latter two isomers have ionization energies well above 9.93 eV and cannot be detected in this study. Therefore, they can be ruled out as source for the trace of  $m/z = 29$ . Based on the ionization energies of  $9.88 \pm 0.07$  eV for  $\text{CH}_2\text{NH}$  and  $8.22 \pm 0.05$  eV for  $\text{CHNH}_2$ , the two isomers can be distinguished by tuning the photoionization energy between these two ionization energies. Figure 3a presents the TPD spectrum of  $m/z = 29$  at 9.93 eV and 9.10 eV photoionization energy. The strong clear peak at 120 K for 9.93 eV vanishes for 9.10 eV (Figure 3a). Based on these findings,  $m/z = 29$  can be assigned to  $\text{CH}_2\text{NH}$ . Therefore, we can conclude that  $\text{CH}_2\text{NH}$  is identified as the product in the radiolysis of  $\text{CH}_3\text{NH}_2$ .

The remaining TPD traces in Figure 3b reveal sublimation maxima at higher temperatures between 135 K and 225 K. Mass-to-charge ratio of 60 represents the heaviest ion detected. It can be attributed to the molecular formula  $C_2N_2H_8$  that can be assigned to four possible isomers:  $NH_2CH_2CH_2NH_2$ , N-Methyl-methanediamine ( $NH_2CH_2NHCH_3$ ), 1,1-dimethylhydrazine ( $(CH_3)_2NNH_2$ ), and 1,2-dimethylhydrazine ( $CH_3NHNHCH_3$ ). They can be distinguished *via* their ionization energies (Table 2). Ethylenediamine has the highest ionization energy of 8.27 eV (calculated) and 8.42 eV (experimental) followed by  $NH_2CH_2NHCH_3$  with 8.23 eV. Taking the energy correction of the Stark shift (0.04 eV) and the offset of the theoretical ionization energy (0.04 eV) into account, the ionization energy of  $NH_2CH_2NHCH_3$  and  $NH_2CH_2CH_2NH_2$  are reduced to 8.15 eV and 8.20 eV, respectively. A photon energy of 8.17 eV is employed to distinguish between both isomers. As presented in Figure 3b, no ion counts are detected at 8.17 eV, revealing that most likely  $NH_2CH_2CH_2NH_2$  is formed during irradiation, which effectively contributes to ion counts at  $m/z = 60$  in the 9.93 eV experiment. However, due to the error of  $\pm 0.05$  eV on the calculated ionization energies we cannot rule out  $NH_2CH_2NHCH_3$  entirely, yet. Nevertheless, we find ion masses at  $m/z = 59, 58, 44, 43,$  and  $30$  which simultaneously subliming with  $m/z = 60$ . In comparison to an ethylenediamine photoionization study by Wei et al.<sup>80</sup> we can relate the ion masses in this study to the photofragments of  $NH_2CH_2CH_2NH_2$  (Table 4). These findings confirm the formation of  $NH_2CH_2CH_2NH_2$ .

In summary, the PI-ReTOF-MS study reveals two newly formed molecules in the  $CH_3NH_2$  ices exposed to ionizing radiation:  $CH_2NH$  and  $NH_2CH_2CH_2NH_2$ . Integrating over the signal in the TPD traces of  $m/z = 32$  with and without irradiation helps to extract the fraction of the non-radiolyzed  $CH_3NH_2$  molecules to be  $92 \pm 4$  %. This coincides nicely with the calculated loss of about  $8 \pm 1$  % from the infrared study.

The previous experiment from Bossa et al. already proposed the formation of  $CH_2NH$ . In their photolysis study they found small features in their FTIR study around  $1722\text{ cm}^{-1}$  and  $1683\text{ cm}^{-1}$  which they postulated to originate from amides or aldehydes. Therefore, they related the  $m/z = 59$  during sublimation in the QMS to N-Methyl formamide. In their experiment they used UV flux of  $10^{15}\text{ photons s}^{-1}\text{ cm}^{-2}$ . This flux converts to about  $14\text{ eV molecule}^{-1}$ ,<sup>81</sup> which is in the same region than the energy dose used in this work. Their findings however only suggest the

existence of N-Methyl formamide, based on the QMS data. An isotope study or an analysis of the isomer structure of  $m/z = 59$  as we present it in this study has not been done in their study.

## 5. Discussion

Having confirmed that  $\text{CH}_2\text{NH}$  and  $\text{NH}_2\text{CH}_2\text{CH}_2\text{NH}_2$  are formed in the irradiated ices, we are discussing now possible formation pathways. Holtom et al.<sup>13</sup> revealed that  $\text{CH}_3\text{NH}_2$  can undergo unimolecular decomposition initiated by energy transfer from the impinging electrons. In particular, two hydrogen loss channels can result in either methylamidogen ( $\text{CH}_3\text{NH}$ ) (3a) or  $\text{CH}_2\text{NH}_2$  (4a) (see also Figure 4); in the present experiments. Each of these radicals can emit a hydrogen atom synthesizing  $\text{CH}_2\text{NH}$  (3b and 4b). These routes are highly endoergic with the energy being supplied from the ionizing radiation via inelastic energy transfer processes. Previous infrared studies after Photolysis by Bossa et al.<sup>34</sup> indicated that both formation routes might lead to  $\text{CH}_2\text{NH}$ . These mechanisms were also documented in gas phase studies by Reed et al.<sup>82</sup> utilizing UV photodissociation of  $\text{CH}_3\text{NH}_2$  at 215 nm in a molecular beam. This work revealed the atomic hydrogen loss pathway and formation of methylamidogen ( $\text{CH}_3\text{NH}$ ) (3a), which was enhanced by a factor of three compared to  $\text{CH}_2\text{NH}_2$  (4a). A summary of the reaction pathways discussed in this study are displayed in Figure 4.

A possible formation pathway for the  $\text{NH}_2\text{CH}_2\text{CH}_2\text{NH}_2$  molecule could follow a barrier-less radical-radical reaction *via* the exoergic recombination of two  $\text{CH}_2\text{NH}_2$  radicals (reaction (5)). At low temperatures, these radical-radical recombination pathways are very prominent in interstellar ices, as long as the radicals are next to each other and the recombination geometry is correct. This has been successfully demonstrated for example for the formation of ethane ( $\text{CH}_3\text{CH}_3$ ),<sup>15, 83, 84</sup> hydrazine ( $\text{NH}_2\text{NH}_2$ ),<sup>85</sup> diphosphine ( $\text{PH}_2\text{PH}_2$ ),<sup>48</sup> hydrogen peroxide ( $\text{HOOH}$ ),<sup>86, 87</sup> ethylene glycol ( $\text{HOCH}_2\text{CH}_2\text{OH}$ ),<sup>41</sup> and hydroxylamine ( $\text{NH}_2\text{OH}$ ),<sup>50</sup> *via* recombination of methyl ( $\text{CH}_3$ ), amido ( $\text{NH}_2$ ), phosphino ( $\text{PH}_2$ ), hydroxyl ( $\text{OH}$ ), and amido ( $\text{NH}_2$ ) with hydroxyl ( $\text{OH}$ ).

Ogura et al.<sup>88</sup> suggested a pathway in analogy to reaction (5). In their gas phase study, they photolyzed gas mixtures of  $\text{CH}_4$ ,  $\text{NH}_3$  and  $\text{H}_2\text{O}$  with broadband UV with highest fluxes at 185 and 254 nm. They detected among others  $\text{NH}_2\text{CH}_2\text{CH}_2\text{NH}_2$ . It should be stressed that the overall reactions to form  $\text{CH}_2\text{NH}$  and  $\text{NH}_2\text{CH}_2\text{CH}_2\text{NH}_2$  from  $\text{CH}_3\text{NH}_2$  are endoergic by  $536 \text{ kJ mol}^{-1}$  (reaction (6)) and  $463 \text{ kJ mol}^{-1}$  (reaction (7)), respectively. Therefore, these reactions cannot

happen thermally at 10 K or during the warm up phase, but have to involve non-equilibrium chemistry.<sup>40</sup> Even a hypothetical molecular hydrogen elimination (reaction (8)) is still endoergic by 104 kJ mol<sup>-1</sup>. Therefore, the reaction pathways involved demand for the presence of an external energy source provided by, e.g., secondary electrons generated by GCRs in order to successfully form the product in the ISM.

## 6. Conclusion

The present study explored the formation of CH<sub>2</sub>NH *via* the unimolecular decomposition of CH<sub>3</sub>NH<sub>2</sub> in interstellar ices. Methylamine is present in several interstellar clouds such as Sagittarius B2<sup>23</sup> and Orion-KL<sup>1, 24</sup> and expected to be incorporated in interstellar ices as well. Even though it is expected that CH<sub>3</sub>NH<sub>2</sub> is present only as minor component in the ice, the present experiments reveal that each CH<sub>2</sub>NH product can result from fragmentation of one single CH<sub>3</sub>NH<sub>2</sub> molecule. These results of our mechanistical studies are transferable to interstellar ice mixtures containing CH<sub>3</sub>NH<sub>2</sub>, which are exposed to ionizing radiation. The irradiation dose utilized in this study is equivalent to 10<sup>5</sup> years of the life time of a cold molecular cloud.<sup>89</sup> Here, CH<sub>2</sub>NH represents an important intermediate to the abiotic formation of extraterrestrial amino acids in interstellar ices,<sup>14</sup> which are essential building blocks for life on Earth.<sup>90</sup> The data collected by the elegant PI-ReTOF-MS approach highlight the feasibility of next generation laboratory studies to detect radiation and reaction products of non-equilibrium chemistries in interstellar analog ices isomer selectively. In addition to the formation of CH<sub>2</sub>NH, the experiments confirmed the formation of NH<sub>2</sub>CH<sub>2</sub>CH<sub>2</sub>NH<sub>2</sub> in the irradiated CH<sub>3</sub>NH<sub>2</sub> ice. This has not been observed in the interstellar medium up to date. A possible explanation might be found by the lower fractional abundance of the parent molecule CH<sub>3</sub>NH<sub>2</sub> in the interstellar ices compared to our analog ice samples. This delimits CH<sub>3</sub>NH<sub>2</sub> molecules present in direct neighborhood to each other in the ice and thus the recombination of two subsequently formed CH<sub>2</sub>NH<sub>2</sub> radicals via radical-radical reaction is delimited as well. As presented earlier, methylamine and CH<sub>2</sub>NH are present in several molecular clouds and star forming regions as well as the dust samples collected by the Stardust mission<sup>4</sup> and the comet 67P/Churyumov-Gerasimenko.<sup>29</sup> Ethylenediamine has not been observed in the interstellar medium or in the Solar System yet, but our results suggest that it should be detectable in those environments where CH<sub>3</sub>NH<sub>2</sub> and CH<sub>2</sub>NH have been discovered. The upper limits of CH<sub>2</sub>NH and of

$\text{NH}_2\text{CH}_2\text{CH}_2\text{NH}_2$  in this study are below  $0.09 \pm 0.01$  and  $0.045 \pm 0.005$  molecules  $\text{eV}^{-1}$ , respectively, and these formation efficiency can be utilized in future astrochemical models of non-equilibrium ice chemistry to predict its interstellar abundance.<sup>91</sup>

It is interesting to note that  $\text{CH}_3\text{NH}_2$  is isoelectronic to  $\text{CH}_3\text{OH}$ . Methanol can reach fractions of up to 27 % with respect to  $\text{H}_2\text{O}$  on interstellar ices. Maity et al.<sup>46, 41, 45, 47</sup> irradiated  $\text{CH}_3\text{OH}$  bearing ices at 5 – 10 K by energetic electrons. Here, methanol, which consists of a methyl ( $\text{CH}_3$ ) and a hydroxyl group ( $\text{OH}$ ) (Table 5), has been found to undergo similar reaction routes compared to  $\text{CH}_3\text{NH}_2$ , which in turn carries a methyl ( $\text{CH}_3$ ) and an amine group ( $\text{NH}_2$ ). In the  $\text{CH}_3\text{OH}$  ice the product  $\text{H}_2\text{CO}$  – isoelectronic to  $\text{CH}_2\text{NH}$  – was formed *via* either a methoxy radical ( $\text{CH}_3\text{O}$ ) or a hydroxymethyl radical intermediate ( $\text{CH}_2\text{OH}$ ) *via* unimolecular decomposition pathways (reactions (9) and (10), Table 5). These reactions are in analogy to pathways (3) and (4) in the present study and are endoergic as well. Each pair of analogous reactions has similar Gibbs free energy changes, which may induce the observed same trends of column densities of  $N_{\text{CH}_3\text{NH}_2} > N_{\text{CH}_2\text{NH}}$  and  $N_{\text{CH}_3\text{OH}} > N_{\text{H}_2\text{CO}}$  in Sagittarius B2<sup>92-94</sup>. Likewise, ethyleneglycol ( $\text{OHCH}_2\text{CH}_2\text{OH}$ ) – isoelectronic to  $\text{NH}_2\text{CH}_2\text{CH}_2\text{NH}_2$  - has been found to be synthesized from the hydroxymethyl ( $\text{CH}_2\text{OH}$ ) *via* radical-radical reaction in  $\text{CH}_3\text{OH}$  ices and has been detected in the interstellar medium toward Sgr B2(N-LMH).<sup>95</sup> This radical-radical formation is similar to the formation of  $\text{NH}_2\text{CH}_2\text{CH}_2\text{NH}_2$  (5) *via* the  $\text{CH}_2\text{NH}_2$  in  $\text{CH}_3\text{NH}_2$  ice in this study. Therefore, ethylenediamine is expected to be present in those interstellar environments, where  $\text{CH}_3\text{NH}_2$  and  $\text{CH}_2\text{NH}$  has been observed as well such as toward Sgr(B2).

### Conflicts of interest

There are no conflicts to declare.

### Acknowledgments

The authors acknowledge support from the US National Science Foundation (AST-1505502) to carry out the experiments. Furthermore, we thank the W. M. Keck Foundation for financing the experimental setup. BJS, YLC, and AHHC thank the National Center for High-performance Computer in Taiwan for providing the computer resources in the calculations.



## References

1. J. E. Dickens, W. M. Irvine, C. H. DeVries and M. Ohishi, *Astrophys. J.*, 1997, **479**, 307.
2. S. Chandra, Sakshi, M. K. Sharma and N. Kumar, *Indian J. Phys.*, 2016, **90**, 733-739.
3. M. A. Sephton, *Nat. Prod. Rep.*, 2002, **19**, 292-311.
4. D. P. Glavin, J. P. Dworkin and S. A. Sandford, *Meteorit. Planet. Sci.*, 2008, **43**, 399-413.
5. K. Kvenvolden, J. Lawless, K. Pering, E. Peterson, J. Flores, C. Ponnamparuma, I. R. Kaplan and C. Moore, *Nature*, 1970, **228**, 923.
6. J. R. Cronin and S. Pizzarello, *Adv. Space Res.*, 1999, **23**, 293-299.
7. O. Botta, J. L. Bada and P. Ehrenfreund, *Asteroids, Comets, and Meteors: ACM 2002*, 2002, **500**, 925-928.
8. S. Pizzarello, Y. Huang and M. Fuller, *Geochim. Cosmochim. Ac*, 2004, **68**, 4963-4969.
9. S. Pizzarello, G. W. Cooper and G. J. Flynn, in *Meteorites and the Early Solar System II*, 2006, pp. 625-651.
10. R. I. Kaiser, A. M. Stockton, Y. S. Kim, E. C. Jensen and R. A. Mathies, *Astrophys. J.*, 2013, **765**, 111.
11. G. M. Muñoz Caro, U. J. Meierhenrich, W. A. Schutte, B. Barbier, A. Arcones Segovia, H. Rosenbauer, W. H.-P. Thiemann, A. Brack and J. M. Greenberg, *Nature*, 2002, **416**, 403-406.
12. M. P. Bernstein, J. P. Dworkin, S. A. Sandford, G. W. Cooper and L. J. Allamandola, *Nature*, 2002, **416**, 401-403.
13. P. D. Holtom, C. J. Bennett, Y. Osamura, N. J. Mason and R. I. Kaiser, *Astrophys. J.*, 2005, **626**, 940.
14. D. E. Woon, *Astrophysl. J. Lett.*, 2002, **571**, L177.
15. Y. S. Kim, C. J. Bennett, L.-H. Chen, K. O'Brien and R. I. Kaiser, *Astrophys. J.*, 2010, **711**, 744.
16. C. Zhu, A. M. Turner, M. J. Abplanalp and R. I. Kaiser, *Astrophys. J. Suppl. S.*, 2018, **234**, 15.
17. P. D. Godfrey, R. D. Brown, B. J. Robinson and M. W. Sinclair, *Astrophys. Lett.*, 1973, **13**, 119.
18. B. E. Turner, *Astrophys. J. Suppl. S.*, 1989, **70**, 539-622.
19. E. C. Sutton, P. A. Jaminet, W. C. Danchi and G. A. Blake, *Astrophys. J. Suppl. S.*, 1991, **77**, 255-285.
20. A. Nummelin, P. Bergman, Å. Hjalmarson, P. Friberg, W. M. Irvine, T. J. Millar, M. Ohishi and S. Saito, *Astrophys. J. Suppl. S.*, 1998, **117**, 427.
21. P. A. Jones, M. G. Burton, M. R. Cunningham, K. M. Menten, P. Schilke, A. Belloche, S. Leurini, J. Ott and A. J. Walsh, *Mon. Not. R. Astron. Soc*, 2008, **386**, 117-137.
22. P. A. Jones, M. G. Burton, N. F. H. Tothill and M. R. Cunningham, *Mon. Not. R. Astron. Soc*, 2011, **411**, 2293-2310.
23. B. E. Turner, R. Terzieva and E. Herbst, *Astrophys. J.*, 1999, **518**, 699.
24. G. J. White, M. Araki, J. S. Greaves, M. Ohishi and N. S. Higginbottom, *Astron. Astrophys.*, 2003, **407**, 589-607.
25. S.-L. Qin, Y. Wu, M. Huang, G. Zhao, D. Li, J.-J. Wang and S. Chen, *Astrophys. J.*, 2010, **711**, 399.
26. E. D. Tenenbaum, J. L. Dodd, S. N. Milam, N. J. Woolf and L. M. Ziurys, *Astrophysl. J. Lett.*, 2010, **720**, L102.

27. C. J. Salter, T. Ghosh, B. Catinella, M. Lebron, M. S. Lerner, R. Minchin and E. Momjian, *Astron. J.*, 2008, **136**, 389.
28. V. Vuitton, R. V. Yelle and M. J. McEwan, *Icarus*, 2007, **191**, 722-742.
29. F. Goesmann, H. Rosenbauer, J. H. Bredehöft, M. Cabane, P. Ehrenfreund, T. Gautier, C. Giri, H. Krüger, L. L. Roy, A. J. MacDermott, S. McKenna-Lawlor, U. J. Meierhenrich, G. M. M. Caro, F. Raulin, R. Roll, A. Steele, H. Steininger, R. Sternberg, C. Szopa, W. Thiemann and S. Ulamec, *Science*, 2015, **349**, aab0689.
30. J. V. Michael and W. A. Noyes, *J. Am. Chem. Soc.*, 1963, **85**, 1228-1233.
31. D. T. Halfen, V. V. Ilyushin and L. M. Ziurys, *Astrophys. J.*, 2013, **767**, 66.
32. M. P. Bernstein, S. A. Sandford, L. J. Allamandola, S. Chang and M. A. Scharberg, *Astrophys. J.*, 1995, **454**, 327.
33. A. Quinto-Hernandez, A. M. Wodtke, C. J. Bennett, Y. S. Kim and R. I. Kaiser, *J. Phys. Chem. A*, 2011, **115**, 250-264.
34. J.-B. Bossa, F. Borget, F. Duvernay, G. Danger, P. Theulé and T. Chiavassa, *Aust. J. Chem.*, 2012, **65**, 129-137.
35. P. Theule, F. Borget, F. Mispelaer, G. Danger, F. Duvernay, J. C. Guillemin and T. Chiavassa, *Astron. Astrophys.*, 2011, **534**, A64.
36. Y. S. Kim and R. I. Kaiser, *Astrophys. J.*, 2011, **729**, 68.
37. G. Socrates, *Infrared and Raman characteristic group frequencies: tables and charts*, John Wiley & Sons, 2001.
38. J. Shu, K. R. Wilson, M. Ahmed and S. R. Leone, *Rev. Sci. Instrum.*, 2006, **77**, 043106.
39. K. R. Wilson, M. Jimenez-Cruz, C. Nicolas, L. Belau, S. R. Leone and M. Ahmed, *J. Phys. Chem. A*, 2006, **110**, 2106-2113.
40. M. J. Abplanalp, S. Gozem, A. I. Krylov, C. N. Shingledecker, E. Herbst and R. I. Kaiser, *P. Natl. Acad. Sci.*, 2016, **113**, 7727-7732.
41. C. J. Bennett, S.-H. Chen, B.-J. Sun, A. H. H. Chang and R. I. Kaiser, *Astrophys. J.*, 2007, **660**, 1588.
42. R. T. Garrod, S. L. W. Weaver and E. Herbst, *Astrophys. J.*, 2008, **682**, 283.
43. E. Herbst and E. F. van Dishoeck, *Annu. Rev. Astron. Astr.*, 2009, **47**, 427-480.
44. C. Walsh, E. Herbst, H. Nomura, T. J. Millar and S. W. Weaver, *Faraday. Discuss.*, 2014, **168**, 389-421.
45. S. Maity, R. I. Kaiser and B. M. Jones, *Faraday. Discuss.*, 2014, **168**, 485.
46. S. Maity, R. I. Kaiser and B. M. Jones, *Phys. Chem. Chem. Phys.*, 2015, **17**, 3081-3114.
47. A. Bergantini, S. Góbi, M. J. Abplanalp and R. I. Kaiser, *Astrophys. J.*, 2018, **852**, 70.
48. A. M. Turner, M. J. Abplanalp, S. Y. Chen, Y. T. Chen, A. H. H. Chang and R. I. Kaiser, *Phys. Chem. Chem. Phys.*, 2015, **17**, 27281-27291.
49. M. Förstel, Y. A. Tsegaw, P. Maksyutenko, A. M. Mebel, W. Sander and R. I. Kaiser, *Chemphyschem*, 2016, **17**, 2726-2735.
50. Y. A. Tsegaw, S. Góbi, M. Förstel, P. Maksyutenko, W. Sander and R. I. Kaiser, *J. Phys. Chem. A*, 2017, **121**, 7477-7493.
51. P. Modica and M. E. Palumbo, *Astron. Astrophys.*, 2010, **519**, A22.
52. R. I. Kaiser and P. Maksyutenko, *J. Phys. Chem. C*, 2015, **119**, 14653-14668.
53. M. Atoji and W. N. Lipscomb, *Acta Crystallogr.*, 1953, **6**, 770-774.
54. P. D. Holtom, A. Dawes, M. P. Davis, S. V. Hoffmann, R. J. Mukerji and N. J. Mason, *Radiat. Phys. Chem.*, 2007, **76**, 745-749.
55. C. J. Bennett, C. Pirim and T. M. Orlando, *Chem. Rev.*, 2013, **113**, 9086-9150.

56. D. Drouin, A. R. Couture, D. Joly, X. Tastet, V. Aimez and R. Gauvin, *Scanning*, 2007, **29**, 92-101.
57. B. M. Jones and R. I. Kaiser, *J. Phys. Chem. Lett.*, 2013, **4**, 1965-1971.
58. B. P. Tsal, T. Baer, A. S. Werner and S. F. Lin, *J. Phys. Chem.*, 1975, **79**, 570-574.
59. K. Watanabe, T. Nakayama and J. Mottl, *J. Quant. Spectrosc. Ra.*, 1962, **2**, 369-382.
60. D. W. Berman, D. S. Bomse and J. L. Beauchamp, *Int. J. Mass Spectrom.*, 1981, **39**, 263-271.
61. A. D. Becke, *J. Chem. Phys.*, 1992, **96**, 2155-2160.
62. A. D. Becke, *J. Chem. Phys.*, 1992, **97**, 9173-9177.
63. A. D. Becke, *J. Chem. Phys.*, 1993, **98**, 5648-5652.
64. C. Lee, W. Yang and R. G. Parr, *Phys. Rev. B*, 1988, **37**, 785-789.
65. G. D. Purvis and R. J. Bartlett, *J. Chem. Phys.*, 1982, **76**, 1910-1918.
66. C. Hampel, K. A. Peterson and H.-J. Werner, *Chem. Phys. Lett.*, 1992, **190**, 1-12.
67. P. J. Knowles, C. Hampel and H. J. Werner, *J. Chem. Phys.*, 1993, **99**, 5219-5227.
68. M. J. O. Deegan and P. J. Knowles, *Chem. Phys. Lett.*, 1994, **227**, 321-326.
69. K. A. Peterson, D. E. Woon and T. H. Dunning, *J. Chem. Phys.*, 1994, **100**, 7410-7415.
70. M. J. Frisch, *GAUSSIAN 09, Revision D.01*, 2013.
71. R. I. Kaiser, L. Belau, S. R. Leone, M. Ahmed, Y. Wang, B. J. Braams and J. M. Bowman, *Chemphyschem*, 2007, **8**, 1236-1239.
72. O. Kostko, J. Zhou, B. J. Sun, J. S. Lie, A. H. H. Chang, R. I. Kaiser and M. Ahmed, *Astrophys. J.*, 2010, **717**, 674.
73. R. I. Kaiser, B. J. Sun, H. M. Lin, A. H. H. Chang, A. M. Mebel, O. Kostko and M. Ahmed, *Astrophys. J.*, 2010, **719**, 1884.
74. J. R. Durig, S. F. Bush and F. G. Baglin, *J. Chem. Phys.*, 1968, **49**, 2106-2117.
75. M. J. Abplanalp, M. Förstel and R. I. Kaiser, *Chem. Phys. Lett.*, 2016, **644**, 79-98.
76. A. M. Turner, M. J. Abplanalp and R. I. Kaiser, *Astrophys. J.*, 2016, **819**, 97.
77. M. Förstel, A. Bergantini, P. Maksyutenko, S. Góbi and R. I. Kaiser, *Astrophys. J.*, 2017, **845**, 83.
78. K. Watanabe and J. R. Mottl, *J. Chem. Phys.*, 1957, **26**, 1773-1774.
79. M. T. Bowers, *Gas phase ion chemistry*, Academic Press, 1979.
80. L. Wei, B. Yang, J. Wang, C. Huang, L. Sheng, Y. Zhang, F. Qi, C.-S. Lam and W.-K. Li, *J. Phys. Chem. A*, 2006, **110**, 9089-9098.
81. N. J. Mason, B. Nair, S. Jheeta and E. Szymańska, *Faraday. Discuss.*, 2014, **168**, 235-247.
82. C. L. Reed, M. Kono and M. N. R. Ashfold, *J. Chem. Soc. Faraday T.*, 1996, **92**, 4897-4904.
83. R. I. Kaiser and K. Roessler, *Astrophys. J.*, 1997, **475**, 144.
84. R. I. Kaiser and K. Roessler, *Astrophys. J.*, 1998, **503**, 959.
85. W. Zheng, D. Jewitt, Y. Osamura and R. I. Kaiser, *Astrophys. J.*, 2008, **674**, 1242.
86. W. Zheng, D. Jewitt and R. I. Kaiser, *Astrophys. J.*, 2006, **648**, 753.
87. W. Zheng, D. Jewitt and R. I. Kaiser, *Phys. Chem. Chem. Phys.*, 2007, **9**, 2556-2563.
88. K. Ogura, C. T. Migita and T. Yamada, *J. Photoch. Photobio. A*, 1989, **49**, 53-61.
89. A. G. Yeghikyan, *Astrophysics*, 2011, **54**, 87-99.
90. A. Shimoyama and R. Ogasawara, *Origins. Life Evol. B.*, 2002, **32**, 165-179.
91. C. N. Shingledecker and E. Herbst, *Phys. Chem. Chem. Phys.*, 2018, **20**, 5359-5367.
92. D. Halfen, A. Apponi, N. Woolf, R. Polt and L. Ziurys, *Astrophys. J.*, 2006, **639**, 237.

93. D. Halfen, V. Ilyushin and L. Ziurys, *Astrophys. J.*, 2013, **767**, 66.
94. V. Thiel, A. Belloche, K. Menten, R. Garrod and H. Müller, *Astron. Astrophys.*, 2017, **605**, L6.
95. J. M. Hollis, F. J. Lovas, P. R. Jewell and L. H. Coudert, *Astrophysl. J. Lett.*, 2002, **571**, L59.
96. N. A. Tarasenko, A. A. Tishenkov, V. G. Zaikin, V. V. Volkova and L. E. Gusel'nikov, *B. Acad. Sci. USSR CH+*, 1986, **35**, 2196-2196.
97. V. H. Dibeler, J. L. Franklin and R. M. Reese, *J. Am. Chem. Soc.*, 1959, **81**, 68-73.
98. M. Meot-Ner, S. F. Nelsen, M. F. Willi and T. B. Frigo, *J. Am. Chem. Soc.*, 1984, **106**, 7384-7389.
99. B. Ruscic and H. Bross, *Active Thermochemical Tables (ATcT) values based on ver. 1.122 of the Thermochemical Network*, ATcT.anl.gov, 2016.
100. F. P. Lossing, Y.-T. Lam and A. Maccoll, *Can. J. Chem.*, 1981, **59**, 2228-2231.
101. D. H. Aue and M. T. Bowers, in *Gas Phase Ion Chemistry, Volume 2*, Elsevier, 1979, pp. 1-51.

**Table 1** Parameter for the vacuum ultraviolet light generation used in the present experiments. The uncertainty for VUV photon energies is 0.001 eV.

	Photoionization energy (eV)	9.93	9.10	8.17
	Flux ( $10^{11}$ photons $s^{-1}$ )	$10 \pm 1$	$6 \pm 1$	$15 \pm 1$
$(2\omega_1 - \omega_2)$	Wavelength (nm)	124.9	136.2	151.8
$\omega_1$	Wavelength (nm)	202.316	222.566	249.628
Nd:YAG ( $\omega_1$ )	Wavelength (nm)	532	355	355
Dye laser ( $\omega_1$ )	Wavelength (nm) - dye laser	606.948	445.132	499.265
Dye		Rh 610/Rh 640	C450	C503
$\omega_2$	Wavelength (nm)	532	607	703
Nd:YAG ( $\omega_1$ )	Wavelength (nm) - Nd:YAG	532	532	532
Dye laser ( $\omega_1$ )	Wavelength (nm) - dye laser	-	607	703
Dye		-	Rh610/Rh640	LDS 867
	Nonlinear medium	Kr	Xe	Xe

**Table 2** Calculated adiabatic ionization energies (IE) and relative energies ( $E_{\text{rel}}$ ) of distinct  $\text{CNH}_3$  and  $\text{C}_2\text{N}_2\text{H}_8$  isomers. The ‘3’ superscript indicates a triplet state.

Structure	Molecular Formula	Species	IE <sup>a</sup> (eV)	$E_{\text{rel}}$ <sup>b</sup> (eV)	Literature value IE, (eV)
	$\text{CH}_2\text{NH}$	Methanimine	9.94	0.00	$9.88 \pm 0.07^c$
	$^3\text{CH}_3\text{N}$	Methylimidogen	12.00	2.34	
	$\text{CHNH}_2$	Aminomethylene	8.22	1.54	
	$^3\text{CHNH}_2$	Aminomethylene	10.94	3.01	
	$\text{NH}_2\text{CH}_2\text{NHCH}_3$	N-Methylmethanediamine	8.23	0.23	
	$\text{NH}_2\text{CH}_2\text{CH}_2\text{NH}_2$	Ethylenediamine	8.27	0.00	$8.42 \pm 0.04^d$
	$\text{CH}_3\text{NHNHCH}_3$	1,2-Dimethylhydrazine	7.18	1.28	$7.8 \pm 0.1^e$
	$(\text{CH}_3)_2\text{NNH}_2$	1,1-Dimethylhydrazine	7.24	1.16	$7.29 \pm 0.05^f$

<sup>a</sup> Relative ionization potential by CCSD(T)/CBS with B3LYP/cc-pVTZ zero-point energy correction in eV

<sup>b</sup> Relative energy by CCSD(T)/CBS with B3LYP/cc-pVTZ zero-point energy correction in eV;

<sup>c</sup> Taken from Tarasenko et al., 1986<sup>96</sup>

<sup>d</sup> Taken from Wei et al., 2006<sup>80</sup>

<sup>e</sup> Taken from Dibeler et al., 1959<sup>97</sup>

<sup>f</sup> Taken from Moet-Ner et al., 1984<sup>98</sup>

**Table 3** Infrared absorption features of  $\text{CH}_3\text{NH}_2$ <sup>74</sup> and  $\text{CH}_2\text{NH}$ <sup>34</sup>

Wavenumber ( $\text{cm}^{-1}$ ) from Literature	Wavenumber ( $\text{cm}^{-1}$ ) This study	Vibration mode	Assignment
<b><math>\text{CH}_3\text{NH}_2</math></b>			
3332	3331	$\text{NH}_2$ antisymmetric stretching	$\nu_{10}$
3260	3260	$\text{NH}_2$ symmetric stretching	$\nu_1$
3191	3170	H bonding	
2942	2945	$\text{CH}_3$ degenerate stretching	$\nu_{11}$
2881	2875	$\text{CH}_3$ degenerate stretching	$\nu_2$
2793	2785	$\text{CH}_3$ symmetric stretching	$\nu_3$
1636	1606	$\text{NH}_2$ scissors	$\nu_4$
1500	1493	$\text{CH}_3$ degenerate deformation	$\nu_{12}$
1467	1465	$\text{CH}_3$ degenerate deformation	$\nu_5$
1441	1445	$\text{CH}_3$ symmetric deformation	$\nu_6$
1353	1356	$\text{NH}_2$ twisting	$\nu_{13}$
1182	1142	$\text{CH}_3$ rocking	$\nu_7, \nu_{14}$
1048	1030	CN stretching	$\nu_8$
1005	983	Torsion first overtone	$2\nu_{15}$
955	917	$\text{NH}_2$ wagging	$\nu_9$
<b><math>\text{CH}_2\text{NH}</math></b>			
3144	3120	CH antisymmetric stretching	$\nu_a$
1662	1643	C=N stretching	$\nu (\text{C}=\text{N})$

**Table 4** Species observed and discussed in this works along with their molecular formula, mass-to-charge ratio ( $m/z$ ), ionization energy (IE), appearance energy (AE) of the observed fragments, and the observed peak sublimation temperature, as well as the Gibbs free energy  $\Delta_r G^\circ$

Species	Chemical Formula	$m/z$	IE (eV)	Sublimation peak (K)	$\Delta_r G^\circ$ (kJ mol <sup>-1</sup> )
Hydrogen	H	1			216 <sup>d</sup>
Methanimine	CH <sub>2</sub> NH	29	9.94 <sup>a</sup>	115	97 <sup>d</sup>
Methylimidogen	<sup>3</sup> CH <sub>3</sub> N	29	12.00 <sup>a</sup>		
Aminomethylene	CHNH <sub>2</sub>	29	8.22 <sup>a</sup>		
Aminomethylene	<sup>3</sup> CHNH <sub>2</sub>	29	10.94 <sup>a</sup>		
Methylamidogen	CH <sub>3</sub> NH	30			187 <sup>d</sup>
Aminomethyl	CH <sub>2</sub> NH <sub>2</sub>	30			160 <sup>d</sup>
Methylamine	CH <sub>3</sub> NH <sub>2</sub>	31	8.97 <sup>b</sup>	115	-7 <sup>d</sup>
Ethylamine	CH <sub>3</sub> CH <sub>2</sub> NH <sub>2</sub>	45	8.9 <sup>b</sup>	115/160	
Dimethylamine	CH <sub>3</sub> NHCH <sub>3</sub>	45	8.2 <sup>b</sup>		
Propylamine	CH <sub>3</sub> CH <sub>2</sub> CH <sub>2</sub> NH <sub>2</sub>	59	8.78 <sup>b</sup>		
2-Propananimine	(CH <sub>3</sub> ) <sub>2</sub> CHNH <sub>2</sub>	59	8.72 <sup>b</sup>		
N-Methyl ethanamine	CH <sub>3</sub> CH <sub>2</sub> NHCH <sub>3</sub>	59	8.15 <sup>f</sup>		
N-Methyl-methanediamine	NH <sub>2</sub> CH <sub>2</sub> NHCH <sub>3</sub>	60	8.23 <sup>a</sup>		
Ethylenediamine	NH <sub>2</sub> CH <sub>2</sub> CH <sub>2</sub> NH <sub>2</sub>	60	8.27 <sup>a</sup>	160	
1,2-Dimethylhydrazine	CH <sub>3</sub> NHNHCH <sub>3</sub>	60	7.18 <sup>a</sup>		
1,1-Dimethylhydrazine	(CH <sub>3</sub> ) <sub>2</sub> NNH <sub>2</sub>	60	7.24 <sup>a</sup>		
Protonated methylamine	CH <sub>3</sub> NH <sub>3</sub> <sup>+</sup>	32			
Methylamine isotope	<sup>13</sup> CH <sub>3</sub> NH <sub>2</sub>	32			
Protonated methylamine isotope	<sup>13</sup> CH <sub>3</sub> NH <sub>3</sub> <sup>+</sup>	33			
<b>Photofragments for ethylenediamine and methylamine</b>					
Methylamine	CNH <sub>4</sub> <sup>+</sup>	30	AE = 10.18 <sup>e</sup>	115	
Ethylenediamine	CNH <sub>4</sub> <sup>+</sup>	30	AE = 9.3 <sup>c</sup>	160	
Ethylenediamine	C <sub>2</sub> NH <sub>5</sub> <sup>+</sup>	43	AE = 8.85 <sup>c</sup>	160	
Ethylenediamine	C <sub>2</sub> NH <sub>6</sub> <sup>+</sup>	44	AE = 8.90 <sup>c</sup>	160	
Ethylenediamine	C <sub>2</sub> N <sub>2</sub> H <sub>6</sub> <sup>+</sup>	58 <sup>c</sup>		160	
Ethylenediamine	C <sub>2</sub> N <sub>2</sub> H <sub>7</sub> <sup>+</sup>	59	AE = 9.06 <sup>c</sup>	160	

<sup>a</sup> This work

<sup>b</sup> Taken from Watanabe et al., 1957<sup>78</sup>

<sup>c</sup> Taken from Wei et al., 2006<sup>80</sup>

<sup>d</sup> Taken from Ruscic et al., 2016<sup>99</sup>

<sup>e</sup> Taken from Lossing et al., 1987<sup>100</sup>

<sup>f</sup> Taken from Aue et al., 1979<sup>101</sup>



**Table 5** Comparison of CH<sub>3</sub>NH<sub>2</sub> and CH<sub>3</sub>OH reaction pathways. Data were taken from the NIST Chemistry WebBook and Active Thermochemical Tables

Reaction number	Reaction	$\Delta_R G$
CH <sub>3</sub> NH <sub>2</sub>		
3a	CH <sub>3</sub> NH <sub>2</sub> → CH <sub>3</sub> NH + H	410 kJ mol <sup>-1</sup> ; 4.25 eV
3b	CH <sub>3</sub> NH → CH <sub>2</sub> NH + H	126 kJ mol <sup>-1</sup> ; 1.31 eV
4a	CH <sub>3</sub> NH <sub>2</sub> → CH <sub>2</sub> NH <sub>2</sub> + H	383 kJ mol <sup>-1</sup> ; 3.97 eV
4b	CH <sub>2</sub> NH <sub>2</sub> → CH <sub>2</sub> NH + H	153 kJ mol <sup>-1</sup> ; 1.59 eV
5	CH <sub>2</sub> NH <sub>2</sub> + CH <sub>2</sub> NH <sub>2</sub> → NH <sub>2</sub> CH <sub>2</sub> CH <sub>2</sub> NH <sub>2</sub>	-337 kJ mol <sup>-1</sup> ; -3.50 eV
6	CH <sub>3</sub> NH <sub>2</sub> → CH <sub>2</sub> NH + 2H	536 kJ mol <sup>-1</sup> ; 5.56 eV
7	CH <sub>3</sub> NH <sub>2</sub> + CH <sub>3</sub> NH <sub>2</sub> → NH <sub>2</sub> CH <sub>2</sub> CH <sub>2</sub> NH <sub>2</sub> + 2H	463 kJ mol <sup>-1</sup> ; 4.80 eV
8	CH <sub>3</sub> NH <sub>2</sub> → CH <sub>2</sub> NH + H <sub>2</sub>	104 kJ mol <sup>-1</sup> ; 1.08 eV
CH <sub>3</sub> OH		
9a	CH <sub>3</sub> OH → CH <sub>3</sub> O + H	435 kJ mol <sup>-1</sup> ; 4.51 eV
9b	CH <sub>3</sub> O → CH <sub>2</sub> O + H	82 kJ mol <sup>-1</sup> ; 0.85 eV
10a	CH <sub>3</sub> OH → CH <sub>2</sub> OH + H	396 kJ mol <sup>-1</sup> ; 4.10 eV
10b	CH <sub>2</sub> OH → CH <sub>2</sub> O + H	121 kJ mol <sup>-1</sup> ; 1.25 eV
11	CH <sub>2</sub> OH + CH <sub>2</sub> OH → HOCH <sub>2</sub> CH <sub>2</sub> OH	-350 kJ mol <sup>-1</sup> ; -3.63 eV
12	CH <sub>3</sub> OH → CH <sub>2</sub> O + 2H	517 kJ mol <sup>-1</sup> ; 5.36 eV
13	CH <sub>3</sub> OH + CH <sub>3</sub> OH → HOCH <sub>2</sub> CH <sub>2</sub> OH + 2H	449 kJ mol <sup>-1</sup> ; 4.65 eV
14	CH <sub>3</sub> OH → CH <sub>2</sub> O + H <sub>2</sub>	85 kJ mol <sup>-1</sup> ; 0.88 eV

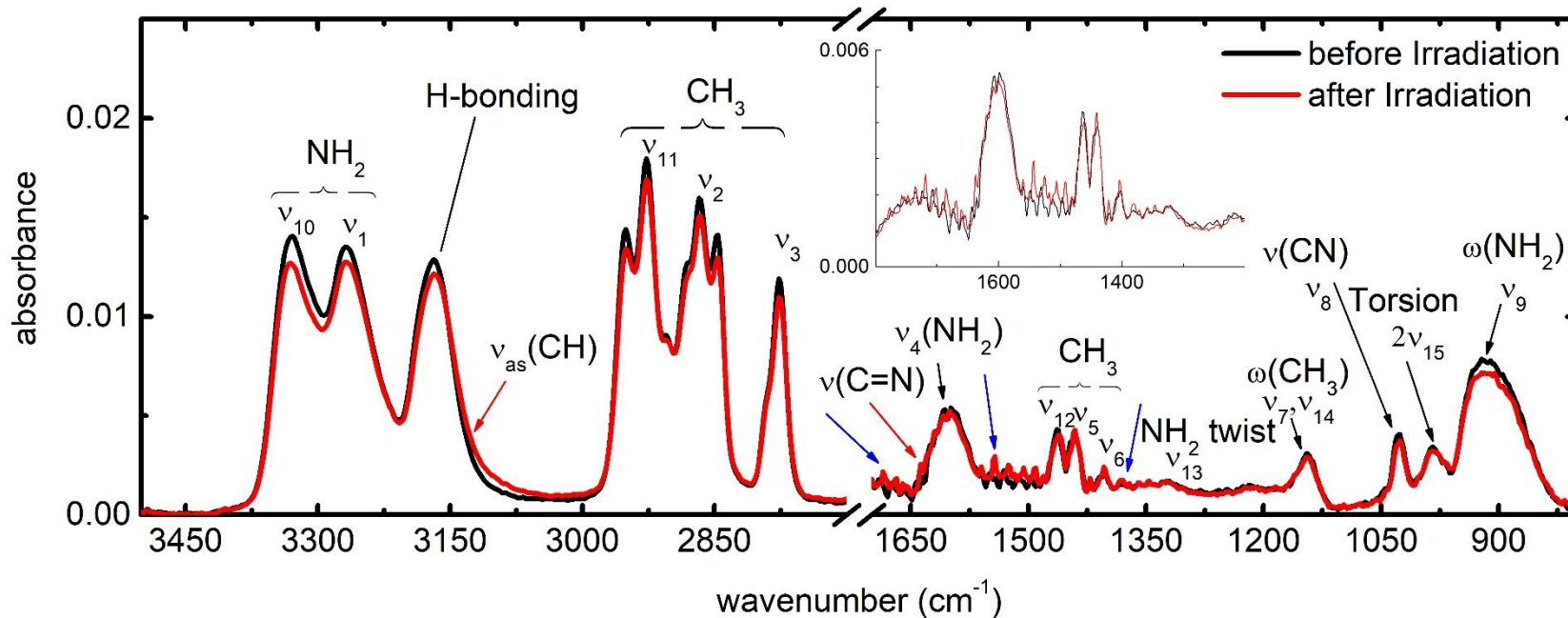


**Figure 1.** FTIR spectra before (black) and after (red) irradiation of the  $\text{CH}_3\text{NH}_2$  ice for the high and low energy region. Besides a loss in total absorbance after irradiation only a few new features are observed. The shoulder around  $3140\text{cm}^{-1}$  and  $1635\text{ cm}^{-1}$  (red arrows) could be tentatively addressed to  $\text{CH}_2\text{NH}$ . Further features at  $1380\text{ cm}^{-1}$ ,  $1540\text{ cm}^{-1}$ , and  $1680\text{ cm}^{-1}$  (blue arrows) cannot be attributed to one particular molecule. Since no features can be found between  $2700$  and  $1700\text{cm}^{-1}$ , these data are not presented, for better display in the relevant regions. The inset expands low-intensity region of the spectra.

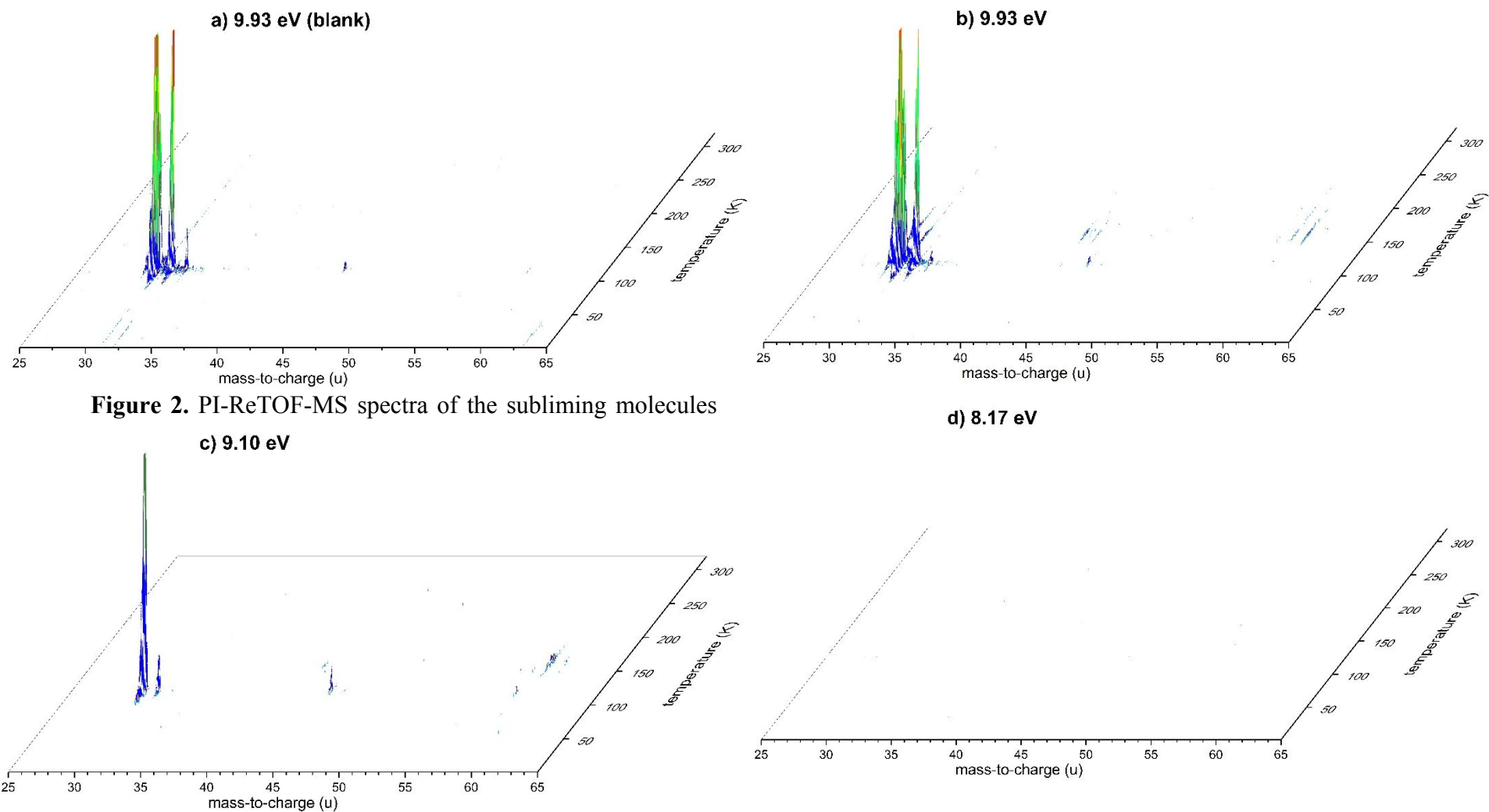


**Figure 2.** PI-ReTOF-MS spectra of the subliming molecules

recorded for the irradiated  $\text{CH}_3\text{NH}_2$  ices obtained at distinct ionization energies. Panel (a) shows the non-irradiated  $\text{CH}_3\text{NH}_2$  ice (blank) while panel (b), (c) and (d) present the irradiated ice analyzed at 9.93 eV, 9.10 eV and 8.17 eV photoionization energy, respectively.

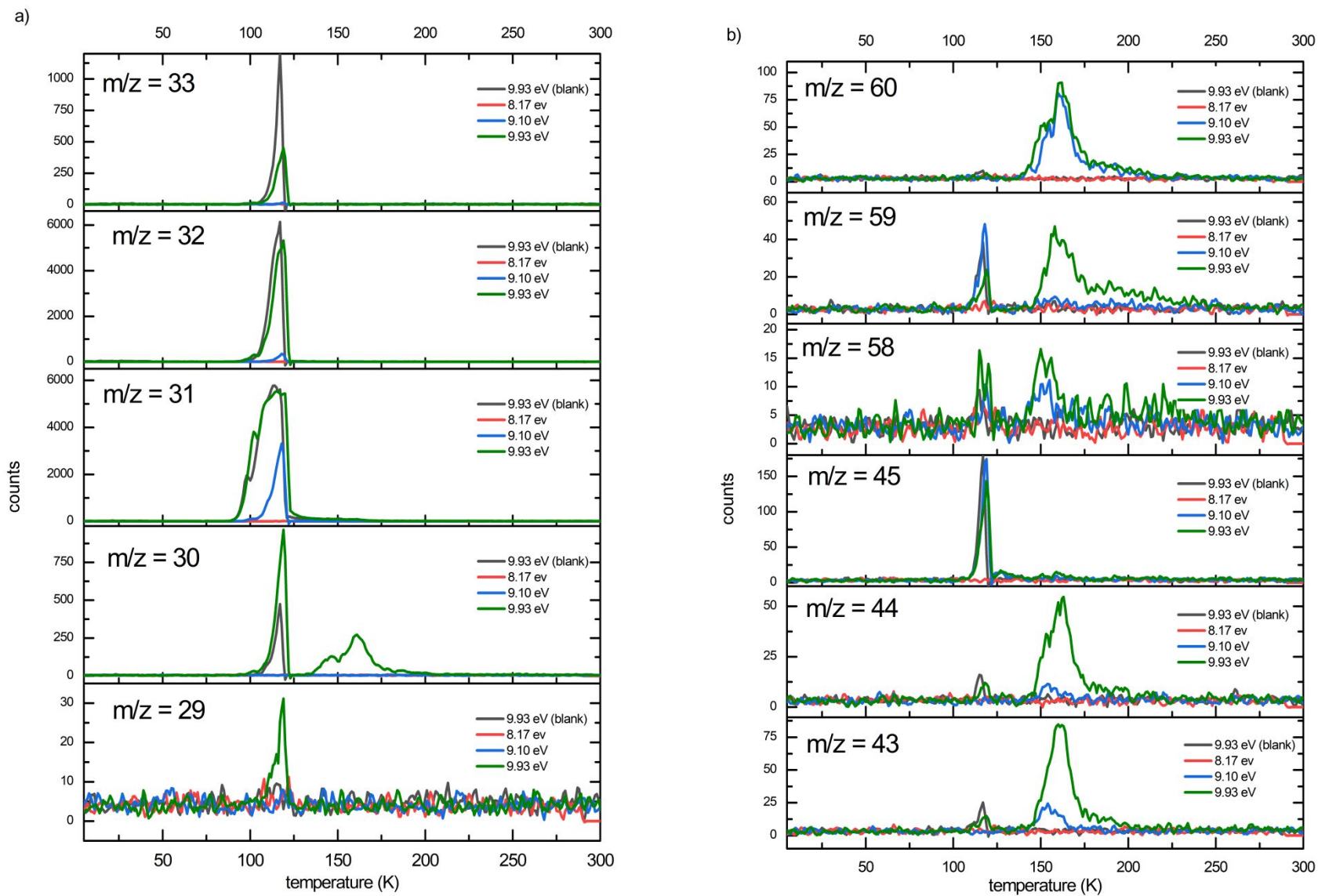


**Figure 3.** TPD traces of lower (a) and higher mass (b) ranges. The  $m/z$  ratio and ionization energy of each trace are given in the legend.

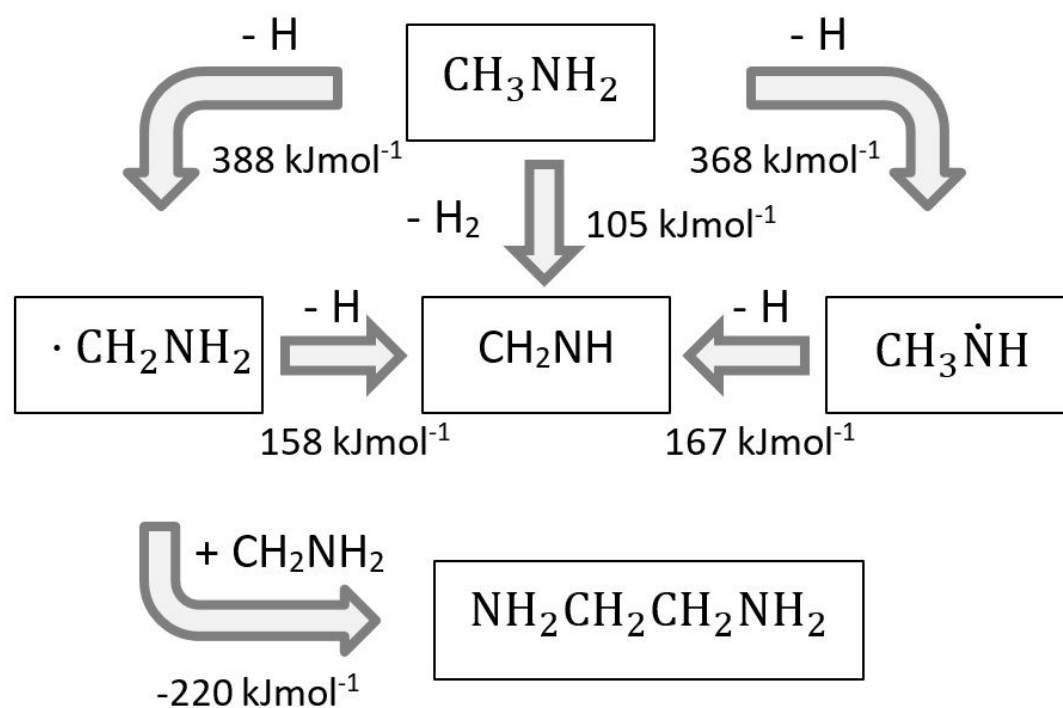


**Figure 4.** Summary of reaction pathways toward  $\text{CH}_2\dot{\text{N}}\text{H}$  and  $\text{NH}_2\text{CH}_2\text{CH}_2\text{NH}_2$ .